Indonesian Journal of Science & Technology 7(1) (2022) 65-88

Indonesian Journal of Science & Technology

Journal homepage: http://ejournal.upi.edu/index.php/ijost/

Aerodynamic Performance of Vertical and Horizontal Axis Wind Turbines: A Comparison Review

Hesam Eftekhari, Abdulkareem Sh. Mahdi Al-Obaidi, Shahrooz Eftekhari*

School of Computer Science and Engineering, Faculty of Innovation,
Taylor's University, No. 1 Jalan SS 15/8 47500 Subang Jaya, Selangor DE, Malaysia
Correspondence: E-mail: abdulkareem.mahdi@taylors.edu.my

ABSTRACT

The need for energy and electricity has been increasing globally, and this means more power is required from the power plants. Power plants, however, will then continue harming the earth because of the greenhouse gasses produced while generating energies that contribute to global warming. Using renewable sources to produce clean energies is one of the sustainable methods to deal with such challenges. Wind energy is one of the renewable sources, which is accessible anywhere on earth, creating green energy. Wind turbines are mainly categorized into Horizontal Axis Wind Turbines (HAWT) and Vertical Axis Wind Turbines (VAWT). This paper firstly presents a general comparison between the HAWTs and VAWTs. Then, it presents mathematical modelling for the aerodynamic factors of HAWT and Darrieus VAWT to assist the researchers to understand some key design aspects of wind turbines, such as lift/drag ratio, tip speed ratio, power coefficient, and torque coefficient. Also, this paper presents a review of the aerodynamic performance of the recent VAWT designs to help researchers to identify and choose the best model among the Savonius and Darrieus rotors for further development or designing a new model at different wind conditions. This comparison review shows that for a large scale HAWT upwind 3 bladed wind turbines are the most optimum. The helical Savonius rotors perform better by having positive torque coefficient at all azimuth angles. Moreover, helical Darrieus was found to produce lesser noise and suitable for conventional areas. hybrid Savonius-Darrieus rotors can solve the self-starting challenge of the VAWTs, and they are suitable at low wind speeds. At last, this review shows some of the recent hybrid Savonius-Darrieus rotors which would help to solve the low efficiency of Savonius rotor and self-starting challenge of Darrieus rotors.

ARTICLE INFO

Article History:
Submitted/Received 03 Oct 2021
First revised 08 Nov 2021
Accepted 11 Jan 2022
First available online 14 Jan 2022
Publication date 01 Apr 2022

Keyword:
HAWT,
Renewable energy,
VAWT,
Wind turbine.

1. INTRODUCTION

Life on Earth for humans is going to be harder and more uncomfortable due to global warming effects. Global warming happens due to the molecular structure of the greenhouse gasses (GHG) which entrap heat in the atmosphere and transfer this heat to the surface of the Earth, as a result, it would further warm the Earth. This cycle of trapping heat causes an overall increment of global temperature. The process is very similar to the way a greenhouse works. Therefore, the gasses that create this effect are named greenhouse gasses (Darkwah *et al*., 2018). Based on the collected data from Enerdata for Global Energy Statistical Yearbook 2020, CO_2 emissions are increasing almost every year globally, which endangers the future of the Earth and human life.

One way to reduce the impact of emissions caused by GHG is to use the renewal energy sources. Clean energy is inevitable, making it interesting for researchers, scientists, and engineers to create other types (Kareem *et al*., 2022; Irawan *et al*., 2021; Putri *et al*., 2021; Sihombing *et al*., 2021; Fauziah *et al*., 2021; Hidayah *et al*., 2021). Wind energy is one of the most well-known renewal energy resources. Wind turbines are used to harvest the wind the energy. The wind turbines' origin is uncertain, but the vertical axis wind rotors were invented around 200 BC in Sistan, Iran. In the twelfth century, Europeans used and modified the Persian Vertical axis wind turbine and then created the traditional European horizontal axis wind rotor (Fleming & Probert, 1984). In 1891, the first horizontal axis wind turbine (HAWT) was designed and constructed in Denmark by La Cour. Later in 1920 first vertical axis wind turbine (VAWT) was patented by a French engineer called Darrieus. La Cour and Darrieus brought the new era for wind turbines, which with the developments through years of research, become the current HAWT and VAWT (Fleming & Probert, 1984). There have been some recent developments on wind turbines (WT).

Components to increase their gearbox and generator efficiency, such as slip rings, brushes, pitch control, bearings, and cables. Wang *et al*., (2008), Habibi & Yousefi-Koma (2014), Jung *et al*. (2017), and Karthikeyan *et al*. (2015) studied different aspects of WT enhancement which in result helped to increase the effective output power of a WT by increasing the aerodynamic efficiency of wind turbines. Aslam Bhutta *et al*. (2012) reviewed the different types of Savonius and Darrieus VAWT and the design methods but did not cover the hybrid Savonius-Darrieus VAWTs. El-Zafry *et al*. (2019) studied all types of VAWTs including the hybrid Savonius-Darrieus but did not cover many variations of each type to decide if there is any variation that has better performance.

All types of wind turbines are developing and the wind turbine machines, in general, are becoming more complex and flexible (Lakhal *et al*., 2017; Fadl *et al*. 2018) but, the HAWT is commonly known and utilized while the VAWT is relatively new and research is being conducted on it due to its advantages over HAWT (Islam *et al*., 2013). An overall comparison between HAWT and VAWT is presented in **Table 1**. Based on previous studies (Anggraeni *et al*., 2020; Al-Obaidi *et al*., 2021; Eftekhari & Al-Obaidi, 2019; Eftekhari *et al*., 2020; Al-Qassar *et al*., 2021; Al-Obaidi, 2021), the main objective of this review is to give a complete and comparative literature survey about the factors affecting the aerodynamics of wind turbines by presenting the mathematical modelling of lift-type wind turbines. This paper intends to serve as a general reference for aerodynamic models and would help as a quick tool in analysing and estimating the aerodynamic properties of HAWT and VAWT. The structure of this review paper is as follows: Section 2 reviews the wind turbines' output power factors and Betz limit. Mathematical relations that are typical for most HAWT models are presented in Section 3. Section 4

DOI: https://doi.org/10.17509/ijost.v7i1
p- ISSN 2528-1410 e- ISSN 2527-8045

shows the typical mathematical relations for VAWT and recent developments on VAWTs designs along with their advantages and disadvantages. Finally, the main contributions followed by the conclusions of this review paper are summarized in Section 5.

2. OUTPUT POWER IN WIND TURBINE

The wind speed is one of the main factors that directly affect the output power of a wind turbine, hence the first step for using a wind turbine in any area is to study and measure the wind speed. The higher wind speed would result in higher output power. This relation can be further understood through Equations [1]-[5]. To calculate the power in the wind or available power for a wind turbine, Equation [1] is used:

$$P_w = \frac{1}{2} \times \rho \times A \times V^3 \quad (1)$$

where ρ is the density of air, *A* is rotor swept area, *V* is wind velocity (Sarkar & Behera, 2012).

The available power for HAWT and VAWT is calculated using Equations [2] and [3] respectively:

$$P_w = \frac{1}{2} \times \rho \times \pi \times R^2 \times V^3 \quad (2)$$

$$P_w = \frac{1}{2} \times \rho \times h \times D \times V^3 \quad (3)$$

where *R* is the radius of HAWT or the length of one blade of HAWT and *h* is the height of the blade, and *D* is the diameter of the VAWT (**Figure 1**). For HAWT construction, the direction of the wind is essential since HAWT interacts with wind from one direction only, while VAWT interacts with wind from different directions which gives an advantage over HAWT. However, the VAWT output power efficiency is known to be lower than HAWT (Akhmedov *et al.*, 2016). To calculate the actual electrical output power of wind turbines produced by a wind turbine, the power coefficient of the wind turbine; also known as the coefficient of performance, must be determined or given (Libii, 2013).

Table 1. Comparison between HAWT and VAWT.

Characteristics	HAWT	VAWT
Electrical energy (Islam *et al.*, 2013)	• Higher electric energy harvesting • Harvest more electric energy from a given amount of wind compared to VAWT.	• Produce up to 50% more electricity on an annual basis versus conventional turbines with the same swept area.
Weight (Islam *et al.*, 2013)	• Heavier	• Lighter
Rotor orientation (Carrigan *et al.*, 2012)	• Horizontal	• Vertical
Wind direction	• Functions at specific wind direction. (Not suitable for turbulent winds)	• Functions in all wind directions. (Suitable for turbulent winds)
Wind speed range (Islam *et al.*, 2013)	• 6 m/s – 25 m/s	• 2 m/s – 65 m/s
Environmental impact (Islam *et al.*, 2013; Rezaeiha *et al.*, 2018)	• Higher chance of bird collision Higher noise	• Lower chance of bird collision Lower noise
Starting function (Feng *et al.*, 2012)	• Higher starting torque • Self-starting	• Lower starting torque • Might require energy to initiate rotation
Variety (Thresher & Dodge, 1999; Tjiu *et al.*, 2015)	• 2 bladed • 3 bladed	• Has two major types with many variations.
Cost and construction (Feng *et al.*, 2012)	• Higher	• Lower

DOI: https://doi.org/10.17509/ijost.v7i1
p- ISSN 2528-1410 e- ISSN 2527-8045

Figure 1. The typical shape of wind turbines: HAWT (left) and VAWT (right).

The captured mechanical energy by the wind blades converts to electrical energy via wind generators. This conversion is influenced by the efficiencies, such as gearbox efficiency, generator efficiency, and electrical efficiency. The total power conversion efficiency from the wind to electricity can be calculated using Equation [4]:

$$\eta_t = C_p \times \eta_{gear} \times \eta_{gen} \times \eta_{ele} \quad (4)$$

where η_t is the total power conversion efficiency, C_p is the power coefficient, η_{gear} is the gear efficiency, η_{gen} is the generator efficiency, and η_{ele} is the electrical efficiency. So, the effective power output from a wind turbine is achieved from Equation [5]:

$$P_{eff} = C_p \times \eta_{gear} \times \eta_{gen} \times \eta_{ele} \times P_w = \eta_t \times P_w \quad (5)$$

where P_{eff} is the effective power output from a wind turbine.

Based on Equations [1]-[5], increasing the conversion efficiency and/or wind power efficiency of the wind turbine helps with the increase of the harvested output power.

Since the air density is almost constant at a given altitude, an increase of the wind power PW can be achieved by increasing the wind speed (by locating the wind turbine in an area with higher wind speed) and/or increasing the swept area of the rotor.

On the other hand, to increase the total power conversion efficiency, one or the combination of the power coefficient, gearbox efficiency, generator efficiency, or electrical efficiency must be increased.

In 1920 Albert Betz (Betz, 2013), a German scientist, formulated the maximum efficiency of an ideal wind turbine rotor, known as 'Betz Limit.' In 1976, Bergey (Bergey, 1979) clarified that a British scientist with the name of Lanchester derived the same maximum in 1915. A Russian aerodynamic scientist, Joukowsky, achieved the same maximum efficiency for an ideal wind turbine in 1920. To honor all of their efforts, this ideal efficiency is known as the 'Lanchester-Betz-Joukowsky limit (Kuik, 2007). Based on this limit, any wind turbine cannot capture more than 59.3% of the available wind energy,

DOI: https://doi.org/10.17509/ijost.v7i1
p- ISSN 2528-1410 e- ISSN 2527-8045

while in practice, the aerodynamic performance reduces due to the tip losses, boundary layer drags, wake, and non-ideal inflow conditions, in other words, $C_{p\ max}$ = 0.593 (Sørensen, 2011). To achieve this limit and to ensure that the disk acts as a drag device that reduces the stream velocity, the following assumptions are to be considered (Ranjbar *et al.*, 2019):

(i) A thin rotor would be replaced by a stationary disc or actuator disc, where it extracts the energy from the passing stream.
(ii) An ideal condition where there is no rotational velocity in the wake.
(iii) The flow is frictionless.
(iv) Now, the general momentum theory shows the performance of disc is as follow Equation [6]:

$$C_P = \frac{P}{\frac{1}{2}\rho V^3 A_D} = 4a(1-a)^2 \tag{6}$$

where A_D is the disc area and a is the induction factor.

The induction factor is expressed using the following Equation [7]:

$$a = \frac{V - V_W}{V} \tag{7}$$

where V_W is the wake velocity in the proximity of the disc, and V is the wind speed.

The maximum value of power coefficient, C_P is achieved from the extremum value of Equation [6], which can be obtained as follows:

$$\frac{dC_P}{da} = 4(1-a)(1-3a) = 0 \tag{8}$$

When an ideal rotor is designed and operated in a way that the wind speed at the rotor is 2/3 of the free-stream wind speed, it is at its maximum power production. So, this means that when $a = \frac{1}{3}$, power production is at maximum, in other words, power coefficient is maximum (Equation [9]):

$$C_{P,max} = \frac{16}{27} = 0.5926 \tag{9}$$

3. HORIZONTAL AXIS WIND TURBINE

HAWT is the most common and popular type of wind turbine because HAWTs are more durable and more efficient than VAWTs. This is why most of the large-scale wind turbines are horizontal-axis types (Wang & Zhuang, 2017). We will be reviewing two major types of HAWT.

3.1 Types of HAWT

There are two types of HAWTs, an upwind wind turbine (UWT) which is a HAWT with blades facing the wind direction, while a downwind wind turbine (DWT) is a HAWT whose blades are facing opposite of wind direction (**Figure 2**). Another difference between these two types is that UWT has a higher power coefficient than DWT. This is due to the design of the DWT which leads to a low power coefficient (Wang *et al.*, 2018).

3.2 Aerodynamics of HAWT

On designing the HAWT with the current technology, three-bladed is the most optimum; the reason behind that lies in a simple comparison between two-, three-, and four-bladed HAWT. Four bladed costs so much that it would not be worth building. These are the reasons why most large-scale WTs are HAWTs with a three-bladed design. The two-bladed design would give the same performance as the three-bladed design by increasing the wind turbine's chord length by 50%. However, then the two-bladed rotate faster than the three-bladed, so it generates more noise, and the two-bladed outstand more stress due to the increment of apparent weight. Moreover, 3-bladed HAWT with 50% peak efficiency (maximum efficiency) is the most efficient WT type among all other type's available WTs (see **Figure 3**) (Schubel & Crossley, 2012).

DOI: https://doi.org/10.17509/ijost.v7i1
p- ISSN 2528-1410 e- ISSN 2527-8045

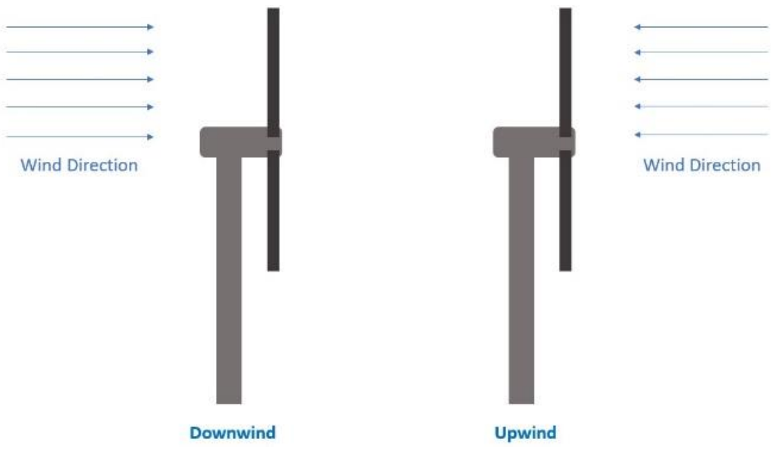

Figure 2. DWT on left and UWT on right.

3.3 Mathematical Framework for HAWT Power Coefficient

Reynolds number Re of airflow over an airfoil is expressed using Equation [10] (Bayati *et al*., 2017).

$$Re = \frac{\rho V_R c}{\mu} = \frac{V_R c}{v} \tag{10}$$

where V_R is the relative airflow velocity, c is the airfoil chord length, μ and v are respectively, the dynamic and kinematic viscosity of air.

The relative airflow velocity V_R for a typical airfoil in a HAWT blade section is expressed in Equation [11].

$$V_R = \sqrt{(V(1-a))^2 + (\Omega r)^2} \tag{11}$$

where V is the free stream velocity, Ω is the angular velocity, r is the radial distance from the center of rotation (Giguère & Selig, 1997).

Airfoil lift forces, drag forces, and lift to drag ratio are presented in Equations [12]-[14] respectively (Manwell *et al*., 2006).

$$L = C_l \frac{1}{2} \rho V^2 A, \tag{12}$$

$$D = C_d \frac{1}{2} \rho V^2 A, \tag{13}$$

$$\frac{L}{D} = \frac{(C_l(0.5)\rho V^2 A)}{(C_d(0.5)\rho V^2 A)} = \frac{C_l}{C_d}. \tag{14}$$

One of the key factors in wind turbine blade design is the tip speed ratio, λ which is calculated using Equations [15] and [16] (Manyonge *et al*., 2014):

$$\mu_O = T \times V \tag{15}$$

$$\lambda = \frac{2\pi R}{\mu_O} \tag{16}$$

where μ_O is the time T taken for one complete oscillation of the rotor blade times the velocity of the wind V and R in Equation [16] is the length of the rotor blade.

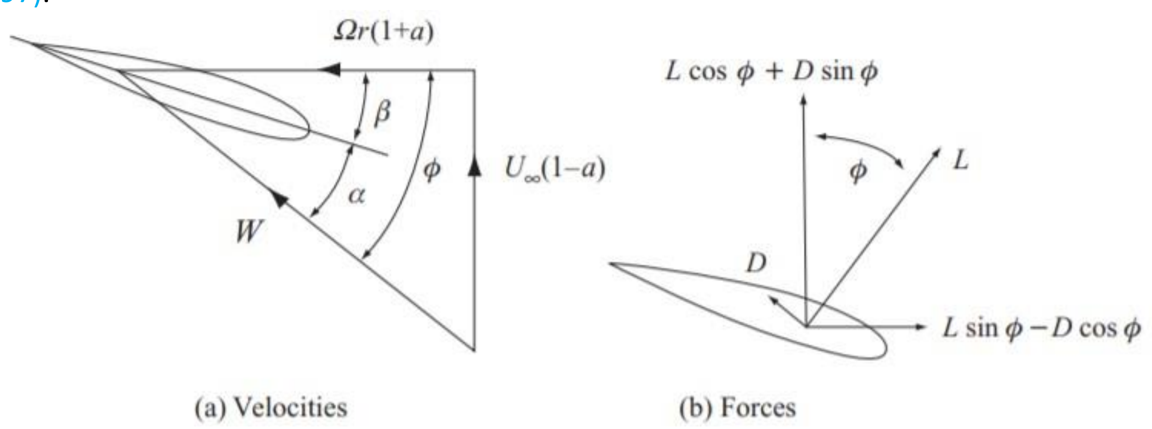

Figure 3. Blade element forces (Left) and velocities (Right) (Leishman, 2011).

DOI: https://doi.org/10.17509/ijost.v7i1
p- ISSN 2528-1410 e- ISSN 2527-8045

The tip speed ratio can also be calculated by division of rotor speed *U* over the wind velocity *V* which is presented in Equation [17] (Malge & Pawar, 2015).

$$\lambda = \frac{U}{V} = \frac{2\pi R}{\mu_O} = \frac{\Omega R}{V} \tag{17}$$

By applying Blade Element Momentum Theory (BEMT), the equations of a wind turbine blade, power-coefficient of the wind turbine can be derived. The BEMT equations are presented in Equations [18]-[22] (Osei *et al.*, 2020).

$$\alpha = \phi - \beta \tag{18}$$

$$\sigma_r = \frac{Bc}{2\pi r} \tag{19}$$

$$\frac{a}{1-a} = \frac{\sigma_r}{4sin^2\phi} \times (C_l cos\phi + C_d sin\phi) \tag{20}$$

$$\frac{a\prime}{1-a\prime} = \frac{\sigma_r}{4sin\phi cos\phi} \times (C_l sin\phi - C_d cos\phi) \tag{21}$$

$$C_P = \frac{8}{\lambda^2}\int_{\lambda_h}^{\lambda} \lambda_r^3 \acute{a}(1-a)\left[1-\left(\frac{C_d}{C_l}\right)cot\phi\right] d\,\lambda_r. \tag{22}$$

where $a'$is the tangential induction factor.

Integrating Equation [22], gives Equation [23] which is a simpler equation to analyze.

$$C_P = \frac{8}{\lambda^2} a'(1 - \frac{C_d}{C_l} cot\phi)(1-a)(\frac{\lambda^4}{4} - \frac{{\lambda_h}^4}{4}) \tag{23}$$

In Equation [23] the relationship between lift to drag ratio and power coefficient of a HAWT is shown. In this equation $\frac{C_d}{C_l}$ is the inverse of lift to drag ratio, so by increasing the lift to drag ratio the expression $(1 - \frac{C_d}{C_l}cot\phi)$ will be larger which results in a higher power coefficient.

Figure 4 shows the flow model used for the BEM analysis of HAWT. Referring to this figure, another approach to the power coefficient of HAWT by using BEMT is expressed in Equations [24] and [25] (Leishman, 2011).

$$r = \frac{y}{R} \tag{24}$$

$$C_p = \sigma\lambda^3 \int_0^1 (\phi C_l - C_d) r^3 dr. \tag{25}$$

Once again in Equation [25], the impact of the lift coefficient in a wind turbine blade design is presented and the importance of a high lift to drag ratio for a wind turbine blade is shown. As it is clear in this equation, with a higher lift coefficient and lower drag coefficient, the power coefficient will increase. So, to design a HAWT blade it is essential to have a high lift to drag ratio airfoil to increase the power coefficient to eventually increase the output power of the wind turbine.

4. VERTICAL AXIS WIND TURBINE

4.1 Major Types

The origin of wind turbines is uncertain, but the start of using wind energy was in Sistan, Iran. Vertical axis wind rotors were invented around 200 BC in Sistan, Iran which was used as a windmill to harvest wind energy (Fleming & Probert, 1984). The 2D design of the vertical axis wind rotor in Sistan is shown in **Figure 5** (Hejazi, 2006).

Generally, the VAWTs come into two major types: Savonius-Rotor, Darrieus-Rotor. Savonius uses drag force to function, similar to the vertical axis windmills that were used in Sistan, and just like HAWTs, they have the self-starting mechanism. However, the Darrieus type mostly needs a starting mechanism since their blade design does not always create sufficient torque for rotation. The Darrius type uses lift force to function which is similar to how the 2-bladed or 3-bladed HAWT works (Tjiu *et al.*, 2015; Wenehenubun *et al.*, 2015, Jadallah *et al.*, 2018). The general shape of the specified type of VAWTs is shown in **Figure 6**.

4.2 Other Configurations of VAWT

One of the advantages of VAWT over HAWT among other advantages is, taking wind from any direction and lower starting torque (Castellani et al., 2019). This advantage is one of the main reasons that the VAWT has more shapes and designs compared to HAWT. Same as HAWT, getting close to the Betz limit is one of the main factors of designing a new VAWT (Yurdusev

DOI: https://doi.org/10.17509/ijost.v7i1
p- ISSN 2528-1410 e- ISSN 2527-8045

et al., 2006). Another reason for coming up with a new or novel shape for a VAWT is to fulfill the design requirement for different geographical conditions such as low wind, high wind speed, urban area, or commercial area. There are several types and configurations of Savonius and Darrieus rotors based on recent research where each of them has its advantages and disadvantages.

The advantages and disadvantages of the various configuration and designs of the Savonius and Darrieus types are presented in **Tables 2** and **3**, respectively. Corresponding figures for different types of Savonius and Darrieus rotors are shown in **Figures 7** and **8**, respectively.

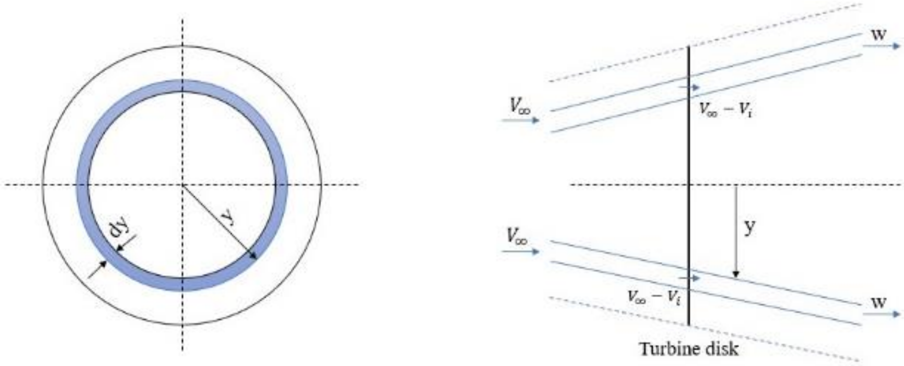

Figure 4. Flow model used for BEM analysis for HAWT. Front view of the disk (Left) and cross-sectional view (right) (Leishman, 2011).

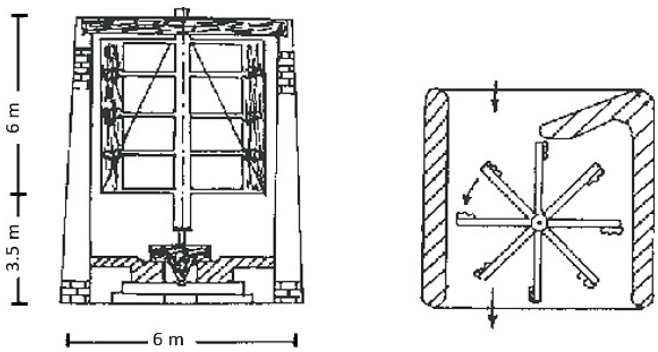

Figure 5. Side view (left) and top view (right) schematic of a windmill in Sistan.

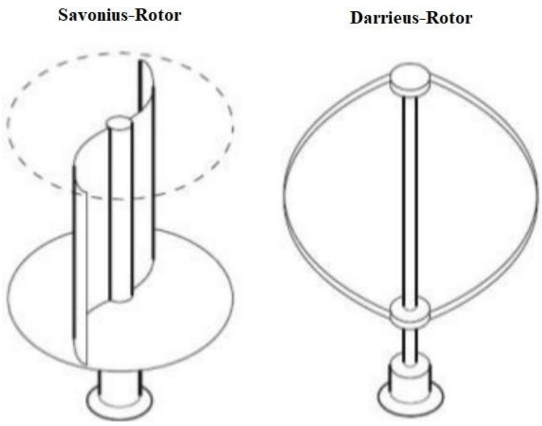

Figure 6. Main types of VAWT (Kumara *et al*., 2017).

DOI: https://doi.org/10.17509/ijost.v7i1
p- ISSN 2528-1410 e- ISSN 2527-8045

It can be concluded from **Tables 2** and **3**, that different researchers tried to improve the efficiency and power coefficient of the VAWTs to reach as close as possible to Betz limit. All these new designs have their advantages and disadvantages, but among the mentioned Savonius rotors, Helical Savonius rotor with full circular end plates had the better performance. Even though the double stage rotors have shown a better performance compared to the single stage, but they take more material and consume more space so would not be suitable for some cases. Using diffusers also increase the performance of the Savonius rotors but they must be placed in a specific location where the wind always comes from a specific direction which could be useful in some special cases where it would be used on top of buildings.

As for the mentioned Darrieus rotors, for large scale, Darrieus Phi rotor is suitable because it has the best performance among the others. For small scale wind turbines to be used in local areas, Helical Darrieus rotors is more suitable because of their steady performance and lower noise compared to straight-bladed and Phi Darrieus rotors.

Table 2. Different configuration of Savonius VAWT advantages and disadvantages.

Configuration	Advantage	Disadvantage
Conventional Savonius rotor (**Figure 7 A**) (Menet & Rezende, 2013)	• Low starting Torque • Low angular velocity • Generating electricity at low and high wind speeds.	• Drag device • Low efficiency
Conventional Savonius rotor with curtains (**Figure 7 B**) (Altan & Atılgan, 2010; B. Altan *et al.*, 2008)	• Best performance at a fixed rotor position $\vartheta = 60º$. • Power coefficient increases by 38% at optimum curtain design. ($\alpha = 45º$ and $\beta = 15º$, $l_1 = 45$cm and $l_2 = 52$cm)	• Change in the curtains angle setting creates negative torque which reduces the power coefficient of the rotor. • Fixed wind direction. • Drag device • Low efficiency
Modified Savonius rotor without shaft (**Figure 7 C**) (Kamoji *et al.*, 2009)	• Higher maximum power coefficient compared to the conventional Savonius rotor with the value of $C_{Pmax} = 0.21$.	• Negative torque coefficient at rotor angles ranging from 135º-165º and 315º-345º. • Drag device • Low efficiency
Conventional Savonius rotor with Combined Conventional and elliptical blade (**Figure 7 D**) (Sanusi *et al.*, 2016)	• The maximum power coefficient of the combined blade is 11% more compared to the conventional blade. • The maximum power coefficient of the combined blade is 5.5% more compared to the elliptical blade.	• Drop-in performance with the use of endplates linking shaft. • Drag device • Low efficiency
Savonius wind turbine with double wind tunnels (**Figure 7 F**) (Promdee & Photong, 2016)	• Generates 45-68% more voltage compared to the conventional Savonius VAWT.	• Only within a specific wind angle range. • Drag device • Low efficiency

DOI: https://doi.org/10.17509/ijost.v7i1
p- ISSN 2528-1410 e- ISSN 2527-8045

Table 2 (Continue). Different configuration of Savonius VAWT advantages and disadvantages.

Configuration	Advantage	Disadvantage
Three-bladed and four-bladed Savonius wind rotor (**Figure 7 G**) (Alit *et al.*, 2017; Saha *et al.*, 2008)	• Three-bladed Savonius rotor higher power coefficient compared to four-bladed.	• The two-bladed Savonius rotor has better performance and a higher power coefficient. • Drag device • Low efficiency
One-stage, Two-stage, and three-stage with 12.5º twisted blade Savonius rotor (**Figure 7 H**) (Saha *et al.*, 2008)	• Twisted blade Savonius rotors have better performance compared to the conventional Savonius rotor due to its positive torque in all rotor angles. • Two-stage twisted Savonius with the Maximum power coefficient of C_{Pmax} = 0.285 has a higher power coefficient compared to one-stage and three-stage.	• Consume more material and more cost for the two-stage and three-stage. • Drag device • Low efficiency

Table 3. Different configurations of Savonius VAWT advantages and disadvantages.

Configuration	Advantage	Disadvantage
Three straight-bladed Darrieus rotors with upper and lower surface connectors. (**Figure 8** A) (Castelli *et al.*, 2011; Jadallah *et al.*, 2018)	• Exceed Betz limit 3 times during one rotor revolution.	• Lower average power coefficient compared to conventional three straight bladed Darrieus rotor.
Straight-bladed Darrieus rotor with upstream deflector. (**Figure 8** B) (Stout *et al.*, 2017)	• At a 90º deflector angle, the maximum power coefficient is C_{Pmax} = 0.20367 which is 1.3% higher compared to the original model.	• Only suitable for wind with a specific wind direction. • Reduced power coefficient at different deflector angles.
Side by side twin straight bladed Darrieus rotor (**Figure 8** C) (Zanforlin and Nishino, 2016; Jin *et al.*, 2020)	• Twin straight-bladed Darrieus rotor has a higher maximum power coefficient compared to the isolated (single) straight-bladed rotor. • Configuration *A* has a higher maximum power coefficient compared to configuration *B*. • $C_{max} \approx 0.493$ with a gap ratio of 1.2 and phase angle of 60º and a TSR of 1.4.	• Suitable for small-scale wind turbines.
Three V-shape blade Darrieus rotor (**Figure 8** D) (Su *et al.*, 2020)	• Both V-shape and inverted V-shape has higher maximum power coefficient compared to the straight blade. • When $\Delta V = 0.6\ c$, power coefficient increases by 20%. • The increment of the power coefficient is mostly on the middle section of the V-shape blade.	• Same as straight-bladed, the V-Shape blade there is energy loss on the blade tip region.

DOI: https://doi.org/10.17509/ijost.v7i1
p- ISSN 2528-1410 e- ISSN 2527-8045

Table 3 (Continue). Different configurations of Savonius VAWT advantages and disadvantages.

Configuration	Advantage	Disadvantage
Darrieus Phi rotor (eggbeater/curved rotor) (**Figure 8** E) (Islam *et al*., 2008; Tjiu *et al.*, 2015)	• With the curvature ratio of 1, it has the highest maximum power coefficient of C_{Pmax} ≈ 0.5. • Cost-effective.	• Rotor height limitation. • Uneven wind velocity on the rotor blades.
Cross axis helical Darrieus rotor (**Figure 8** F) (Muzammil *et al.,* 2017)	• Collect wind energy from horizontal and vertical directions. • Suitable for low wind speed areas.	• Not suitable for high wind speed areas. • Suitable for small-scale wind turbines.
Helical twist Darrieus rotor (**Figure 8** G) (Patel and Sapariya, 2017; Ali *et al*., 2019)	• Steady output power during once rotor oscillation. (□Cp ≈0) • Lower noise compares to • straight-bladed, therefore more suitable, and safer for local areas.	• Lower Max power coefficient compared to the straight-bladed • Darrieus and twisted bladed Darrieus rotors.
Straight blade Darrieus with wingtip devices (**Figure 8** H) (Mishra *et al*., 2020)	• Higher lift with the endplates, therefore better aerodynamic efficiency. • Winglets decrease the induced drag.	• The end plates make the trailing vortices weaker. • Winglets increase the total drag.
J-shaped straight Darrieus (**Figure 8** I) (Zamani *et al*., 2016)	• Improves the self-starting ability. • Less turbulency and noise. • Remove the pressure side of the blades from the maximum thickness to the thrilling edge.	• Generates drag because of the J shaped blades
H-type Darrieus VAWT rotor with winglets (**Figure 8** J) (Cai *et al*., 2019)	• The power coefficient with winglet increased by 10-19% compared to the typical H-type rotor. • More output torque at all azimuth angles compared to the typical H-type rotor. • Aerodynamic performance was improved near the region of the blade tips.	• Adding the winglet could change the optimum TSR slightly. • Doesn't change the performance for every azimuth angle for each of the blades.
Darrieus Phi rotor (troposkien shape) with 50% shifted troposkien shape-VAWT & 100% shifted troposkien shape-VAWT (**Figure 8** K) (Hilewit *et al*., 2019)	• Model A achieved a higher max power coefficient compared to model B and the conventional phi rotor. • Model A performs better at a higher TSR range compared to model B and the conventional phi rotor. • Model B performs better at a higher TSR range compared to the conventional phi rotor. • Lesser cost on model A and model B.	• Reduce blade wake interactions on both models compared to the conventional phi rotor.

DOI: https://doi.org/10.17509/ijost.v7i1
p- ISSN 2528-1410 e- ISSN 2527-8045

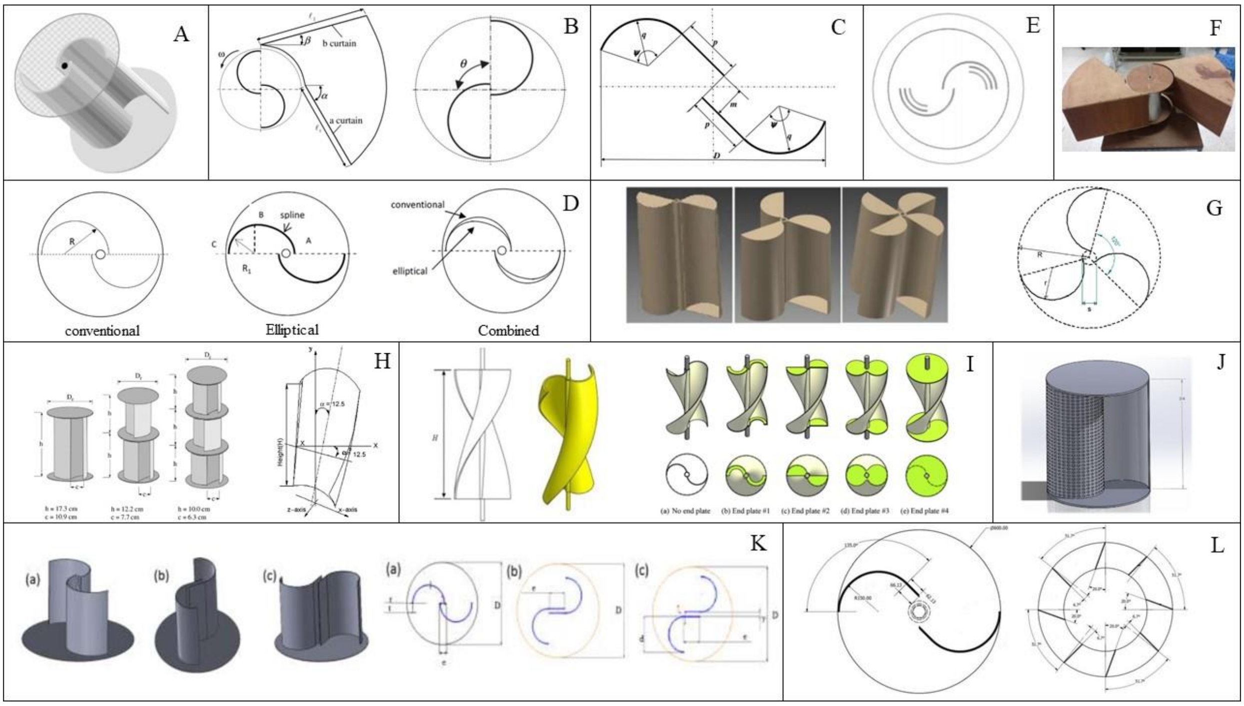

Figure 7. Different configurations of Savonius rotor.

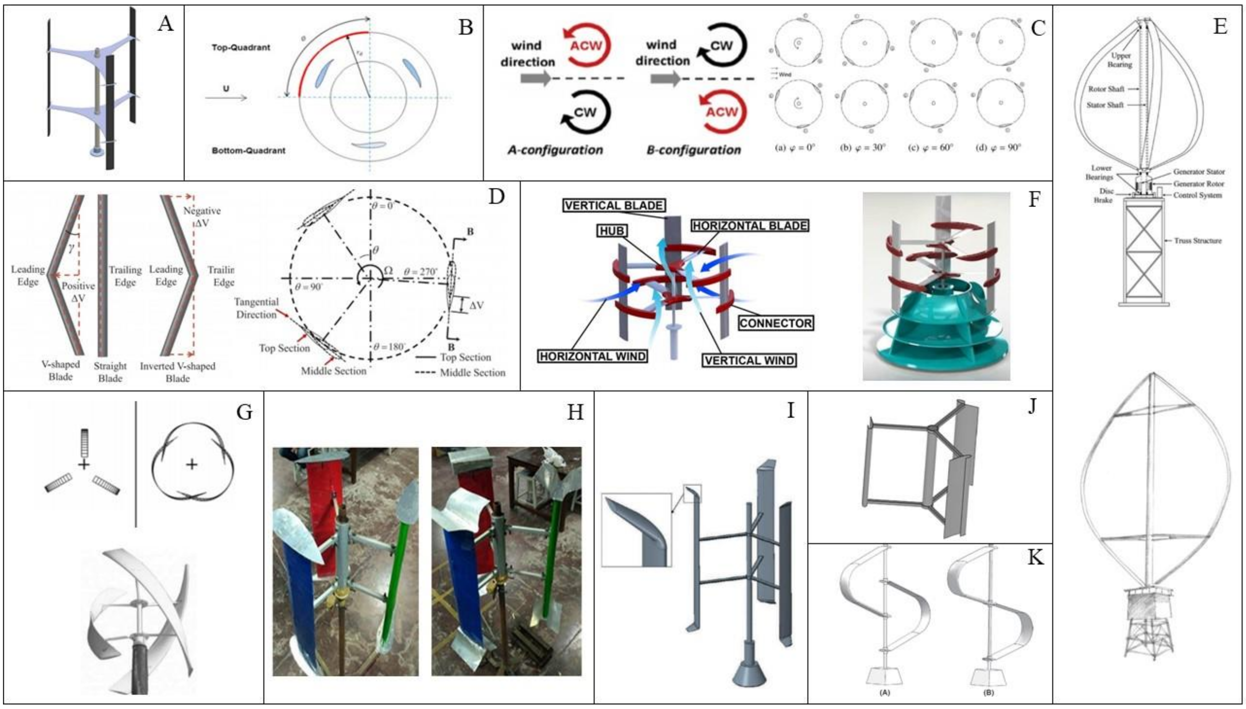

Figure 8. Different configurations of Darrieus rotor.

4.3 Aerodynamics of VAWT

Among VAWTs, the Darrieus types are more efficient and can produce more energy. The main reason is because they have a higher power coefficient (see **Figure 9**). The other difference between the Savonius and Darrieus types is that the Savonius rotors start at lower wind speed, while the Darrius type starts at higher wind speed. However, in terms of aerodynamic performance, the Darrius type is more efficient than the Savonius type since the Darrius type has a higher power coefficient (Aslam Bhutta *et al*., 2012).

DOI: https://doi.org/10.17509/ijost.v7i1
p- ISSN 2528-1410 e- ISSN 2527-8045

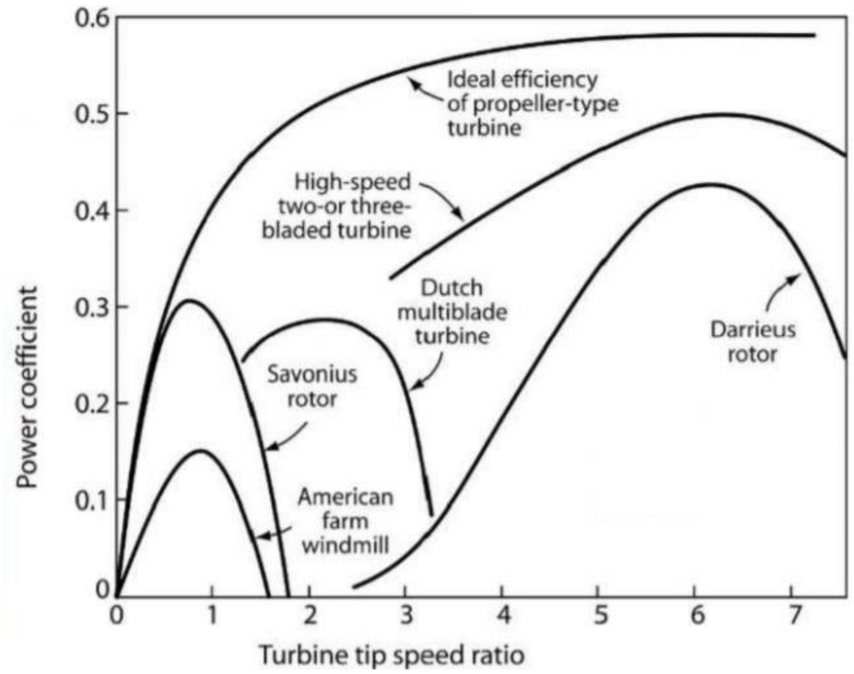

Figure 9. Power coefficient for different wind power generators (Damota *et al.*, 2015).

4.4 Mathematical Framework for VAWT Power Coefficient

VAWT with a lower aspect ratio can achieve a higher power coefficient. **Figure 10** shows the difference between a low and high aspect ratio VAWT. The aspect ratio of a VAWT blade can be found with Equation [26] where *h* is the height of the VAWT blade and *R* is the radius of the VAWT (Brusca *et al.*, 2014).

$$AR_{WT} = \frac{h}{R} \tag{26}$$

From **Figure 11**, the relative airflow velocity V_R and induced velocity V_a are shown in Equations [27]-[29], wind speed is used to express the relative airflow velocity in nondimensional form.

$$V_R = \sqrt{(V_a sin\theta)^2 + (\omega R + V_a cos\theta)^2} \tag{27}$$

$$V_a = V(1 - a) \tag{28}$$

$$\frac{V_R}{V} = \sqrt{((1-a)sin\theta)^2 + (\lambda + (1-a)cos\theta)^2} \tag{29}$$

where V_a is the induced velocity, ω is angular velocity and R is the radius of the turbine, and θ is the azimuth angle. The normal coefficient C_n and tangential coefficient C_t are expressed in Equations [30] and [31].

$$C_n = C_l cos\alpha + C_d sin\alpha \tag{30}$$

$$C_t = C_l sin\alpha - C_d cos\alpha \tag{31}$$

In these equations, α is the angle of attack which can be calculated by Equation [32].

$$\alpha = tan^{-1}[\frac{V_a sin\theta}{\omega R + V_a cos\theta}] \tag{32}$$

Now by using Equations [17] and [28] into Equation [32]:

$$\alpha = tan^{-1}[\frac{(1-a)sin\theta}{\lambda + (1-a)cos\theta}] \tag{33}$$

There are three common momentum models for single-bladed VAWTs of Darrieus type which are the Single StreamTube model (SST), Multiple StreamTube Model (MST), and Double Multiple StreamTube model (DMST). Among these three models, DMST is the best model because in this model vertical and horizontal velocity variations are considered across the stream tube while in the SST model the velocity is constant. Even though in the MST model the velocity varies but the effect of the upwind part and downwind part is not considered. That is why the DMST is the most complete model among these (Amin Mohammed *et al.*, 2019). **Figure 12** shows the difference between these stream tube models.

DOI: https://doi.org/10.17509/ijost.v7i1
p- ISSN 2528-1410 e- ISSN 2527-8045

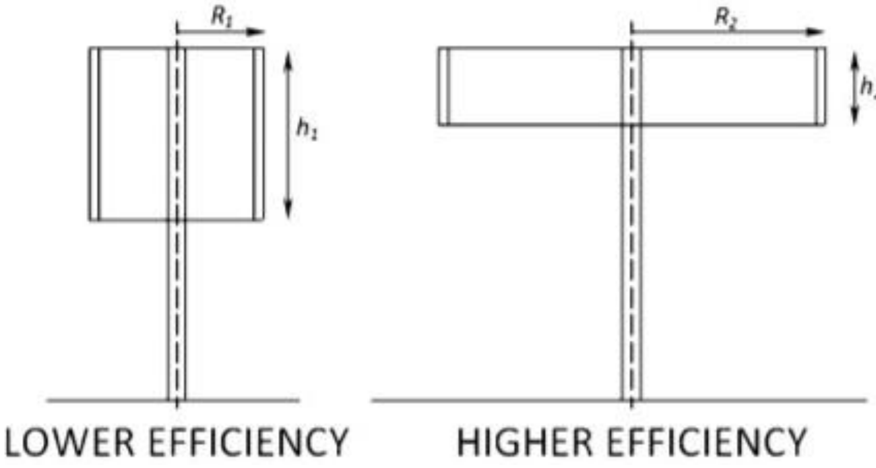

Figure 10. VAWT with different aspect ratios (Brusca *et al.*, 2014).

Double actuator disks are required to be positioned in series as is shown in **Figure 13**. The velocity of the wind at the downstream equilibrium is V_e Now the induced velocity for both upwind V_a and downwind V_a^d are expressed in Equations [34]-[37] (Mohammed *et al.*, 2019).

$$V_a = V(1-a) = \frac{V-V_e}{2} \quad (34)$$

$$V_e = V(1-2a) \quad (35)$$

$$V_a^d = V(1-2a)(1-a^d) = \frac{V_e+V_w^d}{2} \quad (36)$$

$$a^d = \frac{V_e-V_a^d}{V_e} \quad (37)$$

As it is shown in **Figure 14**, the upwind side and downwind side are separated which means it will need 2 different equations to find the power coefficient of the upwind section and the power Coefficient of the downwind section and the total power coefficient will be the summation of these two. Now for the upwind section ($\frac{\pi}{2} \leq \theta \leq \frac{3\pi}{2}$), the relative velocity V_R and the angle of attack α is:

$$V_R = \sqrt{(V_a sin\theta)^2 + (\omega R + V_a cos\theta)^2} \quad (38)$$

$$\alpha = tan^{-1}[\frac{(1-a)sin\theta}{\lambda+(1-a)cos\theta}]. \quad (39)$$

Then for the downwind section ($\frac{3\pi}{2} \leq \theta \leq \frac{\pi}{2}$), the relative velocity V_R^d and the angle of attack is:

$$V_R^d = \sqrt{(V_a^d sin\theta)^2 + (\omega R + V_a^d cos\theta)^2} \quad (40)$$

$$\alpha^d = tan^{-1}[\frac{(1-a^d)sin\theta}{\lambda+(1-a^d)cos\theta}]. \quad (41)$$

The power coefficient of the upwind C_{P_u}, the power coefficient of the downwind C_{P_d}, and the total power coefficient C_P can be determined by Equations [42]-[44] respectively (Mohammed *et al.*, 2019).

$$C_{P_u} = \frac{NcH}{2\pi A}\int_{\frac{\pi}{2}}^{\frac{3\pi}{2}} C_t(\frac{V_R}{V})^2 d\theta, \quad (42)$$

$$C_{P_d} = \frac{NcH}{2\pi A}\int_{\frac{\pi}{2}}^{\frac{3\pi}{2}} C_t(\frac{V_R^d}{V})^2 d\theta, \quad (43)$$

$$C_P = C_{P_u} + C_{P_d}. \quad (44)$$

In both Equations [42] and [43] C_t is one of the main factors, by referring to Equation [31] can notice the importance of high lift to drag ratio airfoils on designing a VAWT Darrieus type.

4.5 Hybrid (Combined) Savonius-Darrieus VAWT

Darrieus rotors have good aerodynamic performance but usually are not self-starting, while the Savonius rotors are self-starting but have low aerodynamic performance because the Savonius rotors will function with drag forces. A combination of them or in other words hybrid Savonius-Darrieus rotor will help to solve the self-starting challenge for the Darrieus rotor and the low aerodynamic performance of the Savonius rotor (Liang *et al.*, 2017). The advantages and disadvantages of the various configuration and designs of the hybrid Savonius-Darrieus are presented in **Table 4**.

DOI: https://doi.org/10.17509/ijost.v7i1
p- ISSN 2528-1410 e- ISSN 2527-8045

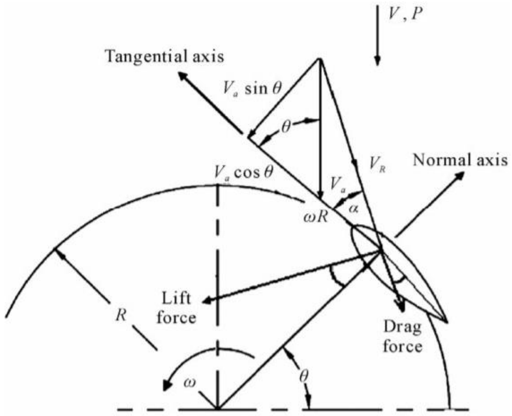

Figure 11. Airfoil velocity and force diagram (Yao, 2011).

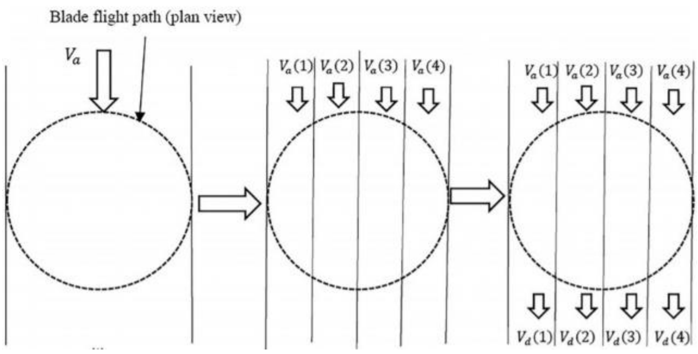

Figure 12. Development of stream tube theory; SST in the (left), MST in the (middle) and DMST in the (right) (Mohammed & Mustafa, 2013)

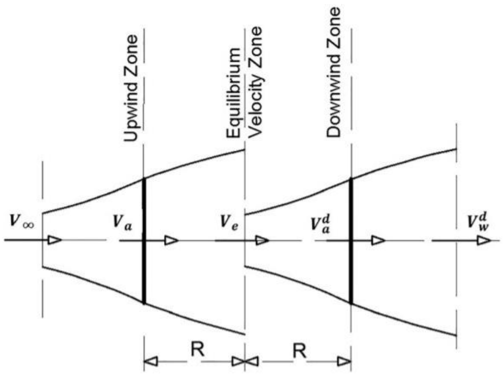

Figure 13. Schematic of the two-actuator disk in tandem (Simonović *et al*., 2013).

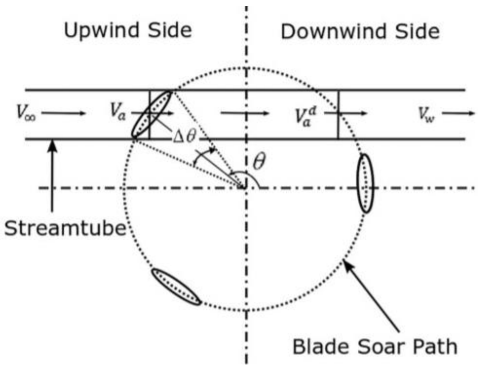

Figure 14. Diagrammatic representation of DMST model (Mohammed *et al*., 2019).

DOI: https://doi.org/10.17509/ijost.v7i1
p- ISSN 2528-1410 e- ISSN 2527-8045

Based on **Table 4**, the self-starting challenge of the Darrieus rotors were solved by mixing them with Savonius rotors, they will have lesser performance compared to the Darrieus rotors. A factor which must be considered while making a hybrid Savonius-Darrieus rotor is the Savonius rotor should be placed inside the Darrieus rotor, because it extracts the wind better at short duration and it is more compact. Among the mentioned hybrid Savonious-Darrieus Two-bladed Savonius with three-bladed helical Darrieus is the most recommended one because the model is not too complex, and the performance is relatively good.

Table 4. Different configuration of hybrid Savonius-Darrieus VAWT advantages and disadvantages.

Configuration	Advantage	Disadvantage
Two-bladed Savonius with three-bladed straight Darrieus (**Figure 15** A) (Nemati, 2020)	• Better performance compared to Darrieus rotor. • It performs well at low TSR. • Unlike the Darrieus rotor, it can function at low wind speed.	• Complex geometry. • Straight Darrieus has better performance.
Two-bladed Savonius with three-bladed helical Darrieus (**Figure 15** B) (Pallotta *et al.*, 2020)	• 20% less starting speed compared to Helical Darrieus alone. (At 3 m/s wind speed) • Higher Performance compared to Savonius rotor alone. • Self-starting.	• 20% performance compares to the Helical Darrieus rotor alone.
Double stages two-bladed Savonius with egg beater Darrieus (**Figure 15** C) (Wakui *et al.*, 2005)	• Type B extracts more output power from wind in small scale and long wind blowing duration, but Type A can extract better in the short wind blowing duration. • Type A is more compact and is more suitable for local areas. • Self-starting.	• Lower output power compares to the Darrieus rotor alone on both models. • Type B has a longer startup time. • Type B has lower performance.
Double stages two-bladed Savonius with two, three, and four-bladed straight bladed Darrieus (**Figure 15** D) (Ahmedov, 2016)	• Better efficiency with three blades compared to two and four-bladed models. • Optimum power coefficient for the hybrid device at 0º. • Self-starting.	• Darrieus rotor alone has better performance and a higher power coefficient. • With 4 Darrieus blades it has better self-starting but a lower maximum power coefficient.
Three-bladed Savonius and thirteen-bladed Darius (**Figure 15** E) (Boz *et al.*, 2020)	• $C_P \approx 0.38$. Better performance compared to Darrieus rotor. Wind focusers (the orange bottom and top section) helped to increase the energy production by 8%. • Self-starting.	• Complex geometry. Costly design due to the complexity of the design and the quantity of the blades.
Combined Bach-type and H-Darrieus rotor (**Figure 15** F) (Hosseini & Goudarzi, 2019)	• $C_{pmax} \approx 0.41$ which is 54% higher than the Savonius rotor alone. • Self-starting.	• Darrieus rotor alone has 17% higher Cpmax compared to the hybrid model • Complex model and higher cost because of the multiple Darrieus and Savonius rotors.

DOI: https://doi.org/10.17509/ijost.v7i1
p- ISSN 2528-1410 e- ISSN 2527-8045

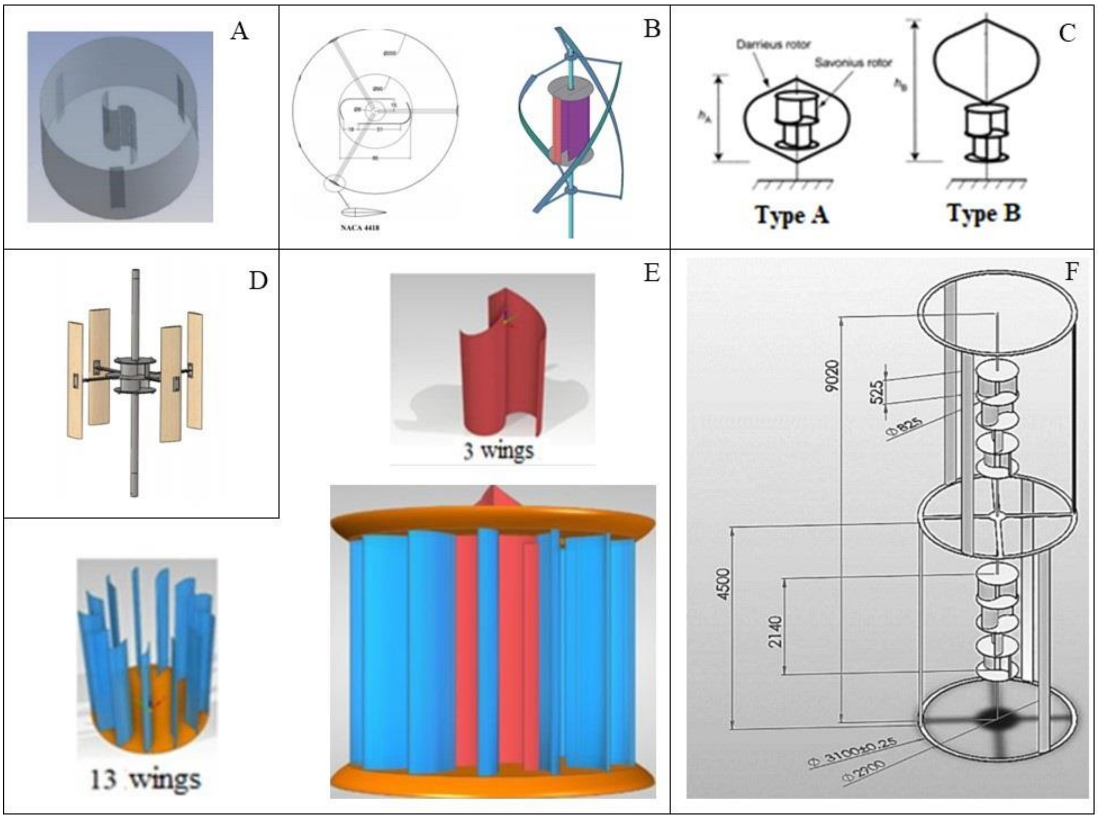

Figure 15. Different configurations of hybrid Savonious-Darrieus rotor.

5. CONCLUSION

The available data on global warming shows the necessity of replacing fossil fuel power plants with green energies. Wind energy is a great solution for the global warming challenge as wind is a free source of energy and it does exist at any place on the earth. Yet choosing the right wind turbine at the right place is always the challenge, because transporting and installing large scale wind turbines is challenging on some locations. Yet using the small scale or micro wind turbines is easier but it is less efficient.

The advantages of HAWTs over the VAWTs are as follow:

- Harvest more energy from a specific wind direction.
- Higher power coefficient.
- Self-starting.

And the VAWTs advantages over the HAWTs are:

- Relatively lesser noise.
- Suitable for turbulent wind.
- Does not harm birds while rotating.
- Less cost for transportations and constructions.
- Can accept wind from all directions.

Based on the findings of this review paper, the following criteria may be used to improve the performance of the Savonius rotors:

- Helical/Twisted blades
- Full circular end plates
- Two-staged blades

As for the Darrieus the following criteria is suggested to performance of the rotor:

(i) Darrieus at low wind speed
  - Cross axis helical Darrieus rotor
  - Side by side twin straight bladed
  - Darrieus rotor
  - Helical twist Darrieus rotor

(ii) Darrieus at high wind speed:
  - Straight-bladed Darrieus
  - Darrieus Phi rotor (eggbeater/curved rotor)

One of the methods to increase solve the self-starting challenge of Darrieus rotors and low efficiency challenge of Savonius rotor is to

DOI: https://doi.org/10.17509/ijost.v7i1
p- ISSN 2528-1410 e- ISSN 2527-8045

use hybrid Savonius-Darrieus rotors. There is so much potential in wind turbine technologies which is yet to be discovered by researchers to achieve as close as possible to Betz Limit to achieve higher power coefficient and in result higher output power from wind turbines.

6. AUTHORS' NOTE

The authors declare that there is no conflict of interest regarding the publication of this article. The authors confirmed that the paper was free of plagiarism.

7. REFERENCES

Ahmedov, A. (2016). *Investigation of the Performance of a Hybrid Wind Turbine Darrieus-Savonius, Abstract of PhD Thesis*. Retrieved on December 2021 from https://www.researchgate.net/publication/323358444_Investigation_of_the_Performance_of_a_Hybrid_Wind_Turbine_Darrieus-Savonius _Abstract_of_PhD_Thesis?channel=doi&linkId=5a8ff4a2aca272140560fca9&showFulltext=true.

Akhmedov, D. S., Eryomin, D. I., Yagfarova, N. I., and Turarbekov, M. K. (2016). Mathematical model to calculate the performance of low power vertical axis wind turbine. *International Journal of Advances in Science, Engineering and Technology*, *4*(1), 23-25.

Ali, N. M., Aljabair, S., and Abdul Hassan, A. K. (2019). An experimental and numerical investigation on Darrieus vertical axis wind turbine types at low wind speed. *International Journal of Mechanical and Mechatronics Engineering IJMME-IJENS*, *19*(06), 97-110.

Alit, I. B., Sutanto, R., Mara, I. M., and Mirmanto, M. (2017). Effect of concentrator, blade diameter and blade number on the savonius wind turbine performance. *Asian Journal of Applied Sciences*, *5*(2), 343-351.

Al-Obaidi, A. S. M. (2021). CDIO initiative: A guarantee for successful accreditation of engineering programmes. *Indonesian Journal of Science and Technology*, *6*(1), 81-92.

Al-Obaidi, A. S. M., Al-Qassar, A., Nasser, A. R., Alkhayyat, A., Humaidi, A. J., and Ibraheem, I. K. (2021). Embedded design and implementation of mobile robot for surveillance applications. *Indonesian Journal of Science and Technology*, *6*(2), 427-440.

Al-Qassar, A. A., Al-Obaidi, A. S. M., Hasan, A. F., Humaidi, A. J., Nasser, A. R., Alkhayyat, A., and Ibraheem, I. K. (2021). Finite-Time control of wing-rock motion for delta wing aircraft based on whale-optimization algorithm. *Indonesian Journal of Science and Technology*, *6*(3), 441-456.

Altan, B. D., Atılgan, M., and Özdamar, A. (2008). An experimental study on improvement of a Savonius rotor performance with curtaining. *Experimental Thermal and Fluid Science*, *32*(8), 1673-1678.

Altan, B., and Atılgan, M. (2010). The use of a curtain design to increase the performance level of a Savonius wind rotors. *Renewable Energy*, *35*, 821-829.

Anggraeni, S., Maulidina, A., Dewi, M.W., Rahmadianti, S., Rizky, Y.P.C., Arinalhaq, Z.F., Usdiyana, D., Nandiyanto, A.B.D. and Al-Obaidi, A.S. (2020). The deployment of drones in

DOI: https://doi.org/10.17509/ijost.v7i1
p- ISSN 2528-1410 e- ISSN 2527-8045

sending drugs and patient blood samples COVID-19. *Indonesian Journal of Science and Technology*, *5*(2),18-25.

Aslam Bhutta, M. M., Hayat, N., Farooq, A. U., Ali, Z., Jamil, S. R., and Hussain, Z. (2012). Vertical axis wind turbine - A review of various configurations and design techniques. *Renewable and Sustainable Energy Reviews*, *16*(4), 1926-1939.

Bayati, I., Belloli, M., Bernini, L., and Zasso, A. (2017). Aerodynamic design methodology for wind tunnel tests of wind turbine rotors. *Journal of Wind Engineering and Industrial Aerodynamics*, *167*, 217-227.

Bergey, K. ~H. (1979). The Lanchester-Betz limit. *Journal of Energy*, *3*, 382-384.

Betz, A. (2013). The Maximum of the Theoretically Possible Exploitation of Wind by Means of a Wind Motor. *Wind Engineering*, *37*(4), 441-446.

Boz, T., Toptas, E., and Bayrak, M. A. (2020). Vertical axis hybrid wind turbine design. *Journal of Mechatronics and Artificial Intelligence in Engineering*, *1*(1), 33-40.

Brusca, S., Lanzafame, R., and Messina, M. (2014). Design of a vertical-axis wind turbine: how the aspect ratio affects the turbine's performance. *International Journal of Energy and Environmental Engineering*, *5*, 1-8.

Cai, X., Zhang, Y., Ding, W., and Bian, S. (2019). The aerodynamic performance of H-type Darrieus VAWT rotor with and without winglets: CFD simulations. *Energy Sources, Part A: Recovery, Utilization, and Environmental Effects*, *41*, 1-12.

Carrigan, T. J., Dennis, B. H., Han, Z. X., and Wang, B. P. (2012). Aerodynamic shape optimization of a vertical-axis wind turbine using differential evolution. *ISRN Renewable Energy*, *2012*, 528418.

Castellani, F., Astolfi, D., Peppoloni, M., Natili, F., Buttà, D., and Hirschl, A. (2019). Experimental vibration analysis of a small-scale vertical wind energy system for residential use. *Machines*, *7*, 35.

Castelli, M. R., Englaro, A., and Benini, E. (2011). The darrieus wind turbine: Proposal for a new performance prediction model based on CFD. *Energy*, *36*(8), 4919-4934.

Damota, J., Lamas, M. I., Couce-Casanova, A., and Rodríguez-García, J. (2015). Vertical axis wind turbines: Current technologies and future trends. *International Conference on Renewable Energies and Power Quality (ICREPQ'15)*, *1*(13), 530-535.

Darkwah, W. K., Odum, B., Addae, M., Koomson, D., Kwakye Danso, B., Oti-Mensah, E., Asenso, T., and Buanya, B. (2018). Greenhouse effect: Greenhouse gases and their impact on global warming. *Journal of Scientific Research and Reports*, *17*, 1-9.

Eftekhari, H., Al-Obaidi, A. S. M., and Eftekhari, S. (2020). The effect of spoiler shape and setting angle on racing cars aerodynamic performance. *Indonesian Journal of Science and Technology*, *5*(1), 11-20.

Eftekhari, S., and Al-Obaidi, A. S. M. (2019). Investigation of a cruising fixed wing mini unmanned aerial vehicle performance optimization. *Indonesian Journal of Science and Technology*, *4*(2), 280-293.

DOI: https://doi.org/10.17509/ijost.v7i1
p- ISSN 2528-1410 e- ISSN 2527-8045

El-Zafry, A., Cairo, Omar, E., El-Hameed, A., Saffaa, M., Hassan, M., and Shaheen, M. (2019). A review on the types of vertical axis wind turbines and the methods of their performance study. *Journal of Multidisciplinary Engineering Science and Technology*, *6*, 10633–10643.

Fadl, A., Abbasher, M., Younis, O., and El seory, A. (2018). A numerical investigation of the performance of wind turbine airfoils with gurney flaps and airfoilshape alteration. Journal *of Engineering Science and Technology* (*JESTEC*), *13*, 1-16.

Fauziah, N. R., Maoludin, S. A., Ramadhan, W. S., Wafi, W., Khoerunnisa, F., Winarno, N. (2021). Geothermal: from education to a new solution for renewable energy. *Indonesian Journal of Multidiciplinary Research, 1*(1), 85-88.

Feng, F., Li, S., Li, Y., and Xu, D. (2012). Torque characteristics simulation on small scale combined type vertical axis wind turbine. *Physics Procedia*, *24*, 781-786.

Fleming, P. D., and Probert, S. D. (1984). The evolution of wind-turbines: An historical review. *Applied Energy*, *18*(3), 163-177.

Giguère, P., and Selig, M. S. (1997). Low reynolds number airfoils for small horizontal axis wind turbines. *Wind Engineering*, *21*(6), 367-380.

Habibi, H., Koma, A. Y., and Howard, I. (2017). Power improvement of non-linear wind turbines during partial load operation using fuzzy inference control. *Journal of Control Engineering and Applied Informatics*, *19*(2), 31-42.

Hejazi, M. (2006). Persian architecture: Conformity with nature in hot-dry regions. *International Journal of Design and Nature and Ecodynamics*, *1*(2), 186-196.

Hidayah, F., Muslihah, F., Nuraida, I., Winda, R., Vania, V., Rusdiana, D. and Suwandi, T. (2021). Steam power plant powered by wood sawdust waste: A prototype of energy crisis solution. *Indonesian Journal of Teaching in Scienc*e, *1*(1), 39-46.

Hilewit, D., Matida, E. A., Fereidooni, A., el Ella, H., and Nitzsche, F. (2019). Power coefficient measurements of a novel vertical axis wind turbine. *Energy Science and Engineering*, *7*(6), 2373-2382.

Hosseini, A., and Goudarzi, N. (2019). Design and CFD study of a hybrid vertical-axis wind turbine by employing a combined Bach-type and H-Darrieus rotor systems. *Energy Conversion and Management*, *189*, 49-59.

Irawan, A. K., Rusdiana, D., Setiawan, W., Purnama, W., Fauzi, R.M., Fauzi, S. A., A. H.F. Alfani, A. H. F., and Arfiyogo, M. R. (2021). Design-construction of a solar cell energy water pump as a clean water source for people in Sirnajaya Village, Gununghalu District. *ASEAN Journal of Science and Engineering Education, 1*(1)*,* 15-20.

Islam, M. R., Mekhilef, S., and Saidur, R. (2013). Progress and recent trends of wind energy technology. *Renewable and Sustainable Energy Reviews*, *21*, 456-468.

Islam, M., Ting, D. S.-K., and Fartaj, A. (2008). Aerodynamic models for Darrieus-type straight-bladed vertical axis wind turbines. *Renewable and Sustainable Energy Reviews*, *12*(4), 1087-1109.

DOI: https://doi.org/10.17509/ijost.v7i1
p- ISSN 2528-1410 e- ISSN 2527-8045

Jadallah, A. A., Farag, S. R., and Hamdi, J. D. (2018). Performance enhancement of a darrius 3-bladed wind turbine using convergent-divergent ducting system. *Journal of Engineering Science and Technology*, *13*(7), 1891-1904.

Jadallah, A. A., Farag, S. R., and Hamdi, J. D. (2018). Performance enhancement of a darrius 3-bladed wind turbine using convergent-divergent ducting system. *Journal of Engineering Science and Technology* (*JESTEC*), *13*(7), 1891-1904.

Jin, G., Zong, Z., Jiang, Y., and Zou, L. (2020). Aerodynamic analysis of side-by-side placed twin vertical-axis wind turbines. *Ocean Engineering*, *209*, 107296.

Jung, C., Schindler, D., Buchholz, A., and Laible, J. (2017). Global gust climate evaluation and its influence on wind turbines. *Energies*, *10*(10), 1474.

Kamoji, M. A., Kedare, S. B., and Prabhu, S. V. (2009). Experimental investigations on single stage modified Savonius rotor. *Applied Energy*, *86*(7), 1064-1073.

Kareem, K., Rasheed, M., Liaquat, A., Hassan, A.M.M., Javed, M.I. and Asif, M. (2022). Clean energy production from jatropha plant as renewable energy source of biodiesel. *ASEAN Journal of Science and Engineering*, *2*(2), 193-198.

Karthikeyan, N., Kalidasa Murugavel, K., Arun Kumar, S., and Rajakumar, S. (2015). Review of aerodynamic developments on small horizontal axis wind turbine blade. *Renewable and Sustainable Energy Reviews*, *42*, 801-822.

Kuik, G. (2007). The lanchester-betz-joukowsky limit. *Wind Energy*, *10*, 289-291.

Kumara, E. A. D., Hettiarachchi, N., and Jayathilake, R. (2017). Review paper: Overview of the vertical axis wind turbines. *International Journal of Scientific Research and Innovative Technology*, *4*, 2313-3759.

Lakhal, Y., Fatima Zahra, B., and El Bakkali, L. (2017). The efficiency of bond graph approach for a flexible wind turbine modeling. *Journal of Engineering Science and Technology* (*JESTEC*), *12(11)*, 2990-3010.

Leishman, J. (2011). Aerodynamics of horizontal axis wind turbines. *Environmental Science and Engineering (Subseries: Environmental Science)*, *1*, 1-69.

Liang, X., Fu, S., Ou, B., Wu, C., Chao, C. Y. H., and Pi, K. (2017). A computational study of the effects of the radius ratio and attachment angle on the performance of a Darrieus-Savonius combined wind turbine. *Renewable Energy*, *113*, 329-334.

Libii, J. N. (2013). Comparing the calculated coefficients of performance of a class of wind turbines that produce power between 330 kw and 7,500 kw. *World Transactions on Engineering and Technology Education*, *11*, 36-40.

Malge, A. M., and Pawar, P. M. (2015). Analysis of lift and drag forces at different azimuth angle of innovative vertical axis wind turbine. *International Journal of Energy Engineering*, *4*(5-8), 12-16.

Manwell, J. F., McCowan, J. G., and Rogers, A. L. (2006). Wind energy explained: Theory, design and application. *Wind Engineering*, *30*(2), 169.

Manyonge, A., Ochieng, P., and Oduor, A. (2014). Mathematical analysis of tip speed ratio of a wind turbine and its effects on power coefficient. *International Journal of Mathematics and Soft Computing*, *4*, 61-66.

Menet, J. L., and de Rezende, T. (2013, August). Static and dynamic study of a conventional Savonius rotor using a numerical simulation. *21è Congrès Français de Mécanique (CFM)*. Retrieved on December 2021 from https://www.researchgate.net/publication/262142912_Static_and_dynamic_study_of_a_conventional_Savonius_rotor_using_a_numerical_simulation

Mishra, T., Jain, A., Nair, A., Khanna, B., and Mitra, S. (2020). Numerical and experimental investigations on a dimpled savonius vertical axis wind turbine. *International Journal of Renewable Energy Research*, *10*(2), 646-653.

Mohammed, A. A., and Mustafa, V. (2013). An easily programmable analysis approach for vertical axis wind turbines. *The Eighth Asia-Pacific Conference on Wind Engineering*, *4*(2), 10-14.

Mohammed, A. A., Ouakad, H. M., Sahin, A. Z., and Bahaidarah, H. (2019). Vertical axis wind turbine aerodynamics: summary and review of momentum models. *Journal of Energy Resources Technology*, *141*(5), 050801.

Muzammil, W. K., Wong, K. H., Chong, W. T., Gwani, M., Wang, C. T., Poh, S. C., and Wang, X. H. (2017). Design and early development of a novel cross axis wind turbine. *Energy Procedia*, *105*, 668-674.

Nemati, A. (2020). Three-dimensional numerical study of the performance of a small combined savonius-darrieus vertical wind turbine. *Iranian (Iranica) Journal of Energy and Environment*, *11*(2), 163-169.

Osei, E., Opoku, R., Sunnu, A., and Adaramola, M. (2020). Development of high performance airfoils for application in small wind turbine power generation. *Journal of Energy*, *2020*, 1-9.

Pallotta, A., Pietrogiacomi, D., and Romano, G. P. (2020). HYBRI - A combined Savonius-Darrieus wind turbine: Performances and flow fields. *Energy*, *191*, 116433.

Patel, A. R., and Sapariya, P. S. (2017). A review on the performance of helical darrieus vertical axis wind turbine. *International Journal of Novel Research and Development*, *2*(4), 52-54.

Promdee, C., and Photong, C. (2016). Effects of wind angles and wind speeds on voltage generation of savonius wind turbine with double wind tunnels. *Procedia Computer Science*, *86*, 401-404.

Putri, B. M., Ningrum, L., Maulida, N. M. (2021). Simple micro-hydro uses water as a renewable energy source. *Indonesian Journal of Multidiciplinary Research, 1*(1), 23-28.

Ranjbar, M., Nasrazadani, S., Zanganeh, H., and Gharali, K. (2019). Reaching the betz limit experimentally and numerically. *Energy Equipment and Systems*, *7*(3), 271-278.

Rezaeiha, A., Montazeri, H., and Blocken, B. (2018). Characterization of aerodynamic performance of vertical axis wind turbines: Impact of operational parameters. *Energy Conversion and Management*, *169*, 45-77.

DOI: https://doi.org/10.17509/ijost.v7i1
p- ISSN 2528-1410 e- ISSN 2527-8045

Saha, U. K., Thotla, S., and Maity, D. (2008). Optimum design configuration of Savonius rotor through wind tunnel experiments. *Journal of Wind Engineering and Industrial Aerodynamics*, *96*(8), 1359-1375.

Sanusi, A., Soeparman, S., Wahyudi, S., and Yuliati, L. (2016). Experimental study of combined blade savonius wind turbine. *International Journal of Renewable Energy Research (IJRER)*, *6*(2), 614-619.

Sarkar, A., and Behera, D. K. (2012). Wind turbine blade efficiency and power calculation with electrical analogy. *International Journal of Scientific and Research Publications*, *2*(2), 1-5.

Schubel, P., and Crossley, R. (2012). Wind turbine blade design. *Energies*, *5*(9), 3425-3449.

Sharma, S., and Sharma, R. K. (2016). Performance improvement of Savonius rotor using multiple quarter blades - A CFD investigation. *Energy Conversion and Management*, *127*, 43-54.

Sihombing, D. A., Yulianti, L., Prima E. C. (2021). Aloe vera as an alternative energy source. *Indonesian Journal of Multidiciplinary Research, 1*(1), 29-34.

Sørensen, J. N. (2011). Aerodynamic aspects of wind energy conversion. *Annual Review of Fluid Mechanics*, *43*(1), 427-448.

Stout, C., Islam, S., White, A., Arnott, S., Kollovozi, E., Shaw, M., Droubi, G., Sinha, Y., and Bird, B. (2017). Efficiency Improvement of vertical axis wind turbines with an upstream deflector. *Energy Procedia*, *118*, 141-148.

Su, J., Chen, Y., Han, Z., Zhou, D., Bao, Y., and Zhao, Y. (2020). Investigation of V-shaped blade for the performance improvement of vertical axis wind turbines. *Applied Energy*, *260*, 114326.

Thresher, R. W., and Dodge, D. M. (1999). Trends in the evolution of wind turbine generator configurations and systems. *Wind Energy*, *1*, 70-86.

Tjiu, W., Marnoto, T., Sohif, M., Ruslan, M. H., and Sopian, K. (2015). Darrieus vertical axis wind turbine for power generation I: Assessment of Darrieus VAWT configurations. *Renewable Energy*, *75*, 50-67.

Wakui, T., Tanzawa, Y., Hashizume, T., and Nagao, T. (2005). Hybrid configuration of Darrieus and Savonius rotors for stand-alone wind turbine-generator systems. *Electrical Engineering in Japan*, *150*, 13-22.

Wang, F., Bai, L., Fletcher, J., Whiteford, J., and Cullen, D. (2008). Development of small domestic wind turbine with scoop and prediction of its annual power output. *Renewable Energy*, *33*(7), 1637-1651.

Wang, Z., and Zhuang, M. (2017). Leading-edge serrations for performance improvement on a vertical-axis wind turbine at low tip-speed-ratios. *Applied Energy*, *208*, 1184-1197.

Wang, Z., Tian, W., and Hu, H. (2018). A Comparative study on the aeromechanic performances of upwind and downwind horizontal-axis wind turbines. *Energy Conversion and Management*, *163*, 100-110.

Wenehenubun, F., Saputra, A., and Sutanto, H. (2015). An experimental study on the performance of savonius wind turbines related with the number of blades. *Energy Procedia*, *68*, 297-304.

Yao, H. B. and Y. (2011). Double multiple streamtube model and numerical analysis of vertical axis wind turbine. *Energy and Power Engineering*, *3*(3), 262-270.

Yurdusev, M. A., Ata, R., and Çetin, N. S. (2006). Assessment of optimum tip speed ratio in wind turbines using artificial neural networks. *Energy*, *31*(12), 2153-2161.

Zamani, M., Nazari, S., Moshizi, S. A., and Maghrebi, M. J. (2016). Three-dimensional simulation of J-shaped Darrieus vertical axis wind turbine. *Energy*, *116*, 1243-1255.

Zanforlin, S., and Nishino, T. (2016). Fluid dynamic mechanisms of enhanced power generation by closely spaced vertical axis wind turbines. *Renewable Energy*, *99*, 1213-1226.

DOI: https://doi.org/10.17509/ijost.v7i1
p- ISSN 2528-1410 e- ISSN 2527-8045